ELSEVIER

Polymer 43 (2002) 5903–5914

polymer

www.elsevier.com/locate/polymer

# Crystal structure, morphology, orientation, and mechanical properties of biaxially oriented polyamide 6 films

Sangkeun Rhee[a,*], James L. White[b]

[a]*Specialty Films Division, Honeywell, 101 Columbia Road, Morristown, NJ 07962, USA*
[b]*Institute of Polymer Engineering, The University of Akron, Akron, OH 44325-0301, USA*

Received 26 December 2001; received in revised form 26 June 2002; accepted 8 July 2002

**Abstract**

Investigations on crystal structure, orientation and mechanical properties of extrusion cast and biaxially stretched polyamide 6 films were carried out by using differential scanning calorimetry, wide angle X-ray diffraction, birefringence and tensile testing. The measurements were taken at three stages (1) after extrusion film casting, (2) after film stretching, (3) after solution annealing. Aging unstretched films, which had about 5% crystallinity, at room condition (22–23 °C and 22–31%RH, relative humidity) caused significant elevations in glass transition temperature ($T_g$) cold crystallization temperature ($T_c$) and crystallinity. The melting point ($T_m$) remained almost constant throughout the aging. The room temperature crystal form was investigated. Poorly defined β (or pleated α) crystals were found in the aged films, when they were either unstretched or stretched at low temperature. By increasing the stretch temperature from 40 to 180 °C, the poorly defined β (or pleated α) unit cell from low temperature stretching became similar to the well known α unit cell. Annealing the films, which had been stretched at 65 °C, in boiling 20% formic acid solution perfected the crystal transformation to the well defined α form. We developed a pseudo-orthorhombic unit cell in order to calculate biaxial orientation factors of the crystalline phase. The mechanical properties were successfully correlated with out-of-plane birefringences. © 2002 Published by Elsevier Science Ltd.

*Keywords:* Polyamide 6; Crystals; Aging

## 1. Introduction

Polyamide 6 has been one of the most widely used engineering thermoplastics since the I.G. Farbenindustrie commercially developed it about 1940. It has been largely applied to fibers and molded parts. Biaxially oriented polyamide 6 films also represent a significant proportion in worldwide polymer film production. Polyamide 6 films are biaxially stretched by double bubble film blowing extrusion or extrusion film casting followed by a tentering frame process.

The crystal structure and polymorphism of polyamides have been extensively studied [1–30]. Crystals of aliphatic polyamides are composed in sheet-like structure of hydrogen bonded layers below their Brill transition point [31]. Polyamide 6 has been most widely studied [1,4–6,9,10,12–14,20–23] (Table 1). Polymorphism in room temperature unit cells of polyamide 6 includes α [1,4,6], β [1,4,9,10] (or pleated α [22,23]) and γ [5,13,14,18] unit cells with various sorts of intermediate states [12,20]. All the present crystalline forms of polyamide 6 seem to consist of hydrogen bonded sheets regularly packed in an alternating up-and-down manner, resulting in monoclinic or pseudo-hexagonal symmetry. The β (or pleated α) crystal of polyamide 6, which is generally formed in melt-spun fibers or quenched samples, is identified by a single strong lateral reflection at about 4.2 Å and a strong chain-directional reflection at about 8.5 Å [9,10,21]. The wide-angle X-ray diffraction (WAXD) patterns of the γ crystal are apparently the same as those of the β (or pleated α) crystal. It is generally believed that the β (or pleated α) crystal of polyamide 6 is not very stable and is easily transformed into more stable α [1,4] or γ forms [13] whereas the γ crystal is not transformed to the other forms. The well defined α crystal, which is characteristic of two lateral reflections at about 4.4 Å for α (002) and 3.7 Å for α (200), can be obtained by annealing poorly defined β (or pleated α) crystals at high temperature or in acid type solution. The well-defined γ crystal can be obtained by treating either α or β crystals in iodine-potassium iodide aqueous solution

* Corresponding author. Fax: +1-973-455-4216.
*E-mail address:* rhees11@hotmail.com (S. Rhee).

0032-3861/02/$ - see front matter © 2002 Published by Elsevier Science Ltd.
PII: S0032-3861(02)00489-5

Table 1
Crystal structures of polyamide 6 proposed by various investigators

| Unit cell dimensions | | | | | | Crystal system | Crystal type | Reference |
|---|---|---|---|---|---|---|---|---|
| $a$ (Å) | $b$ (Å) | $c$ (Å) | $\alpha$ (°) | $\beta$ (°) | $\gamma$ (°) | | | |
| 9.60 | 17.2 | 8.32 | 90 | 65 | 90 | Mono | α | [1] |
| 9.56 | 17.24 | 8.01 | 90 | 67.5 | 90 | Mono | α | [4] |
| 9.60 | 17.20 | 9.60 | 90 | 60 | 90 | Mono (or Hexa) | β | [9,10] |
| 4.79 | 16.70 | 4.79 | 90 | 60 | 90 | Mono (or P-hexa) | γ | [13] |
| 9.33 | 16.88 | 4.78 | 90 | 121 | 90 | Mono | γ | [14] |
| 9.56 | 16.88 | 9.56 | 90 | 121 | 90 | Mono | Pleated α | [22,23] |

Crystallographic $b$-axis is the chain axis in the monoclinic symmetry of polyamide 6. (Mono = monoclinic, Hexa = hexagonal, and P-hexa = pseudohexagonal).

followed by removal of the absorbed iodine by sodium thiosulfate [13,14,18].

The molecular orientation of polyamide 6 melt-spun and drawn fibers have been widely studied by various researchers [21,22,26]. Bankar et al. [21] found that the melt-spun polyamide 6 fibers, which are crystallized mainly on the bobbin during storage after spinning process, experienced considerable increase in birefringence with respect to aging time during room temperature storage. However, there have been few studies [32–35] made with polyamide 6 films. The present authors described crystal structure and orientation of double bubble polyamide 6 films in a recent paper [32].

There are no papers containing systematic studies on the crystal structure, polymorphism and molecular orientation of extrusion cast polyamide 6 films which are subsequently biaxially stretched and annealed. We have made a series of investigations with polyamide films (polyamide 6 [32], 612 [36], 11 [37–39] and 12 [37,40,41]) which try to overcome this deficiency. In this paper, we will discuss the effect of stretching conditions (stretch ratio and stretch temperature) and post-stretch annealing on the crystal structure, molecular orientation and mechanical properties of either the unstretched or the stretched extrusion cast polyamide 6 films. This paper is an extension of our earlier studies that have been carried out with polyamide films.

## 2. Experimental

### 2.1. Material

Polyamide 6 homopolymer resin (B135-WP) was provided by Allied Signal Co. (currently Honeywell Speciality Materials). The Newtonian viscosity from a measurement with Rheometrics Mechanical Spectrometer (RMS-800) was $0.82 \times 10^3$ Pa s at 275 °C. This suggests a molecular weight of about 27,000.

### 2.2. Film formation

Absorbed moisture in polyamide 6 resin was dried out in a vacuum oven at 80 °C for more than 24 h. The extrusion film casting utilized a 25 mm Prodex single screw extruder with 203 mm wide sheet casting T-die. The extrusion was carried out at 275 °C. The melt extrudate was quenched with a 14.5 °C chill roll and wound up by take-up device. We stored the extrusion cast film in a refrigerator so that aging of the film was prevented before the stretching operation.

The biaxial stretching operation of the extrusion cast film was carried out with an Iwamoto biaxial stretcher (Model BIX-702) at various temperatures between 40 and 180 °C. The extrusion cast film was immediately stretched right after loading by various stretch ratios at a constant stretching rate of 0.2 $s^{-1}$. The stretch ratio ($\lambda_{TD}/\lambda_{MD} = (L_{TD}/L^0_{TD})/(L_{MD}/L^0_{MD})$) was associated with the changes in length ($L$) from the initial value ($L^0$) along two principal stretch directions (the TD and the MD). The stretched films were heat-set for 4 min in the frame of the biaxial stretching machine at the stretch temperature, cooled down below their glass transition temperature with an air blower and then taken out from the clamps. These steps were important to maintain the dimensions of the stretched films.

### 2.3. Annealing procedures

The unstretched and stretched extrusion cast polyamide 6 films were annealed in a boiling 20% formic acid aqueous solution at 102 °C for 20 min in order to determine the effects of the annealing on the crystal polymorphism and morphology.

### 2.4. Differential scanning calorimetry

Differential scanning calorimetry (DuPont DSC 910) was utilized for determining various thermal properties such glass transition temperature, cold crystallization temperature, melting temperature and crystallinity. Heating scans were made at a constant heating rate of 20 °C/min. The

degree of crystallinity was calculated through

$$X(\%) = \frac{\Delta H_{\text{net}}}{\Delta H^0} \times 100 \quad (1)$$

$$\Delta H_{\text{net}} = \Delta H_{\text{fusion}} - \Delta H_{\text{cold,cry}} \quad (2)$$

where $\Delta H_{\text{fusion}}$ is the heat of fusion and $\Delta H_{\text{cold,cry}}$ the heat of cold crystallization. The heat of fusion ($\Delta H^0 = 190.6\ \text{J/g}$) for a perfect polyamide 6 crystal which was proposed by Inoue [42] was used.

### 2.5. Wide angle X-ray diffraction measurements

The crystal form and orientation of polyamide 6 film samples were investigated by means of WAXD technique at room temperature.

A general electric X-ray generator equipped with a pin-hole type camera generated Cu Kα X-ray radiation at 30 mA and 30 kV for WAXD flat film patterns. The ray was monochromatized with a nickel foil filter. Three photographs were taken for each film sample. They were thru-view (the MD vertical + X-ray beam parallel to the ND), edge-view (the MD vertical + X-ray beam parallel to the TD) and end-view (the TD vertical + X-ray beam parallel to the MD) patterns.

More detailed crystallographic information was also gathered from WAXD diffractometer $2\theta$ scans using a Rigaku X-ray generator model. The Cu Kα X-ray radiation was obtained at 40 kV and 150 mA and filtered by reflecting X-ray beam on the inserted crystal monochromator. The thin film was stacked into a suitable thickness with extreme caution of their directionality.

The $d$-spacing ($= d_{hkl}$) of a successive atomic ($hkl$) plane was calculated with experimentally obtained $\theta_{hkl}$ by using Bragg's law

$$2d_{hkl} \sin \theta_{hkl} = n\lambda \quad (3)$$

where $\lambda$ ( = 1.54178 Å) was the wavelength of Cu Kα X-ray radiation.

The orientation of a specified crystallographic ($hkl$) reflection plane was determined by WAXD pole figure measurements. The Cu Kα X-ray beam was generated from a GE XRD-6 copper target X-ray generator and monochromatized with a crystal monochromator. The X-ray unit was operated at 30 kV and 30 mA. Film samples, which were cut and stacked into a dimension of 1.5 mm × 1.5 mm × 10 mm with the long axis along the MD or the TD, were mounted on an automated single crystal orienter. During the collection of intensity data, the sample was rotated with $\Phi_{i,z}$ (0–90°) at 5° increment. The $z$ crystallographic axis is normal to the ($hkl$) plane of interest. The azimuthal angle $\Phi_{i,z}$ (angle between $z$ axis and $i$ (either the MD or the TD) spindle axis) practically means the angle between the plane consisting of the incident and reflected beams and the spindle axis. At $\Phi_{i,z} = 0$, the spindle axis was horizontal. At each step of $\Phi_{i,z}$ ($> 0$), the longitudinal angle $\kappa_{i,z}$ (0–350°) was rotated by 10° interval from $i$-ND meridian ($\kappa_{i,z} = 0$) around a spindle axis. The intensity $I(\kappa_{i,z}, \Phi_{i,z})$ was automatically recorded by a computer. The data were plotted into two or three-dimensional figures using Surfer Version 6.0 commercialized by Golden Software Inc.

### 2.6. Mechanical properties

Mechanical properties of polyamide 6 film samples were investigated by means of Instron 4204 Tensile Tester at room condition (21–25 °C and 25–31%RH, relative humidity). The testing was generally carried out along the MD and the TD at a cross-head speed of 5 mm/min at room condition. The test samples had been aged more than two weeks at room condition after film formation.

## 3. Results

### 3.1. Stretchability of extrusion cast polyamide 6 films

The extrusion cast film which were obtained by extrusion at 275 °C with a 14.5 °C chill roll was successfully biaxially stretched into films up to a stretch ratio of $\lambda_{\text{TD}}/\lambda_{\text{MD}} = 2.5 : 3.0$ without showing necking propagation when they are not aged. Films aged at room condition (22–23 °C and 22–31%RH) for more than one week showed no ductility and could not be stretched to high extension ratios. Even at an early stage of stretching, serious necking occurred.

### 3.2. Differential scanning calorimetry (DSC) measurements

The unstretched extrusion cast film ($\lambda_{\text{TD}}/\lambda_{\text{MD}} = 1.0 : 1.0$) was aged at 22–23 °C and 22–31%RH in order to investigate changes in thermal properties with respect to the aging time. Fig. 1 gives an indication that the glass transition ($T_g$) and the cold crystallization ($T_c$) temperatures decrease initially from 37 to 62 °C, respectively, at 2 min aging to their minimum values 19 and 40 °C, respectively, and then increase continuously to 40 and 68 °C, respectively, for 1 week aging. The crystallinity increases monotonously from 5% at 2 min aging to 27% at one week aging. The melting temperature ($T_m$) of 220 °C remains throughout aging with little variation. The speed of the changes in thermal properties and their finally achieved values may be dependent upon the environmental humidity. The absorbed moisture may be the cause of an endothermic peak broadly existing above $T_c$ and below the onset of melting.

We have carried out biaxial stretching with the unaged extrusion cast polyamide 6 films at 65 °C at various stretching ratios up to $\lambda_{\text{TD}}/\lambda_{\text{MD}} = 2.5 : 3.0$. The DSC scans of these stretched films, which were made after 2 weeks aging at room environment of 22–23 °C and 22–31%RH, showed widely scattered values of $T_g$ (28–48 °C),

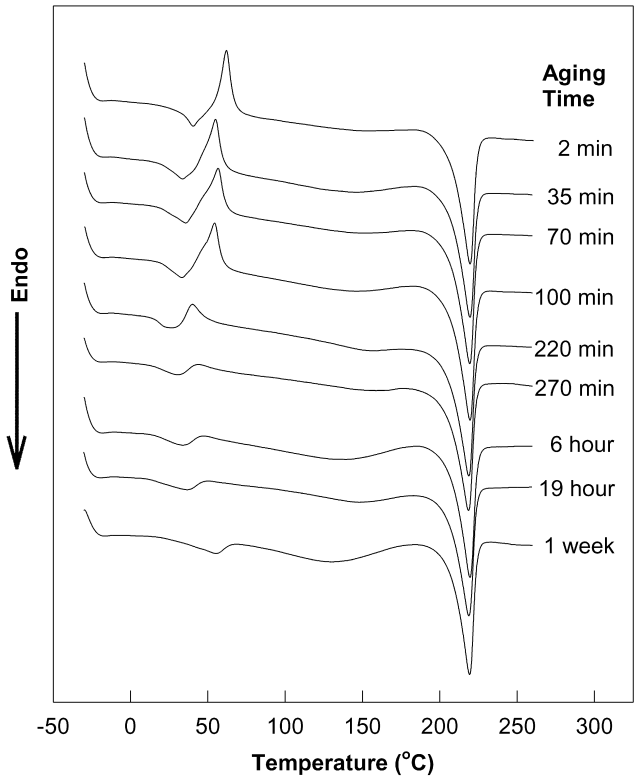


Fig. 1. Thermographs versus aging time of an unstretched extrusion cast polyamide 6 film which is extruded at 275 °C and cooled down with a 14.5 °C chill roll. The environmental condition for this measurement is 22–23 °C and 22–31%RH.

$T_c$ (51–68 °C) and crystallinity (26–31%). This stretching operation made little changes in $T_m$ (220 °C). We were not able to find a general correlation between thermal properties and stretching ratio. By increasing stretch temperature from 40 to 180 °C for unit width stretching ($\lambda_{TD}/\lambda_{MD} = 1.0 : 3.0$), an increase in crystallinity (27% at 40 °C to 33% at 180 °C) was achieved. However, the effects of stretch temperature on $T_g$, $T_c$ and $T_m$ were not clearly found.

### 3.3. WAXD flat film patterns

Fig. 2 presents the WAXD flat film patterns of the unstretched and the stretched extrusion cast polyamide 6 films. The stretched films were made at 65 °C in a stretching operation for various stretch ratios. The unstretched film exhibits single reflection at $d$-spacing of about 4.2 Å and a diffuse ring at about 8.1 Å. When the film is stretched at a unit width ($\lambda_{TD} = 1.0$) to the MD, the reflections at 4.2 and 8.1 Å intensify at the equator and in the MD, respectively. This indicates the development of uniaxial orientation. In the case of biaxially stretched film ($\lambda_{TD}/\lambda_{MD} = 2.5 : 3.0$), one reflection at about 4.3 Å is observed at about 59° tilted from the ND to the MD (in the edge-view) or to the TD (in the end-view). Another reflection at about 3.9 Å of this film has strongest intensity in the ND in both edge- and end-view patterns. Fig. 3 presents typical WAXD film patterns of the films stretched at 65 °C and annealed in a boiling 20% formic acid solution for 20 min. The patterns have three reflections at $d$-spacings of about 4.4, 3.7 and 8.4 Å. In the case of constant width stretching ($\lambda_{TD}/\lambda_{MD} = 1.0 : 3.0$), the 4.4 and 3.7 Å reflections intensify at the equator about the primary stretching direction (the MD) while the 8.4 Å reflection appears along the MD. For biaxially stretched film ($\lambda_{TD}/\lambda_{MD} = 2.5 : 3.0$), two reflections at 4.4 and 3.7 Å are found. Another reflection at about 3.7 Å existing largely tilted from the ND shows weak intensity compared to the one at the ND. Based on these observations and previous investigators [1,4,22,23], we can assign the 4.2–3.7 Å (in the ND), 4.2–4.4 Å (near to the TD) and 8.1–8.4 Å (in the MD) reflections as being the (002), (200) and (020) planes, respectively, of the Brill–Holmes et al.'s [1,4] monoclinic α unit cell.

Changes in the WAXD $2\theta$ scanning patterns of the films having $\lambda_{TD}/\lambda_{MD} = 1.0 : 3.0$ with respect to stretch temperature (40–180 °C) are demonstrated in Fig. 4. The patterns exhibit ($0k0$) reflections in the MD. The reflections having maximum intensity in the TD are mainly attributed to the (200) planes while those in the ND to the (002) planes. Most of the reflections except the one for (402), experiences significant changes in $d$-spacings as shown in Fig. 5. Annealing created further changes in the $d$-spacing. The $d$-spacings for (200) and (002) reflections are more largely separated from each other by annealing as well as by increasing stretch temperature. All $d$-spacings for ($0k0$) reflections increase with the changes.

### 3.4. WAXD pole figure patterns

Intensity maps of X-ray reflections are presented in Fig. 6 for the unannealed and Fig. 7 for the annealed stretched extrusion cast polyamide 6 films as 2-D and 3-D WAXD pole figure patterns. The (002) and (020) reflections of the unannealed films stretched at 65 °C are clearly found in the ND and the MD, respectively. However their (200) reflection, which is supposed to appear at around 60° away from the ND to the TD, is not strong. The annealed films have sharp and distinctive (002) and (200) reflections. The (002) reflection is in the ND for the biaxial case. The (020) reflections are hardly discernable from the background due to a drastic reduction in intensity after the annealing operation.

### 3.5. Birefringences

The in-plane ($\Delta n_{12}$) and out-of-plane ($\Delta n_{13}, \Delta n_{23}$) birefringences of the unannealed stretched extrusion cast polyamide 6 films are given in Fig. 8 in terms of stretch ratio ($\lambda_{TD}/\lambda_{MD}$). The films under this study were stretched at a constant temperature of 65 °C. The $\Delta n_{12}$ and the $\Delta n_{13}$ increase with increasing $\lambda_{MD}$ at a constant $\lambda_{TD}$. In the case of unit width stretching ($\lambda_{TD} = 1.0$), the $\Delta n_{23}$ remains

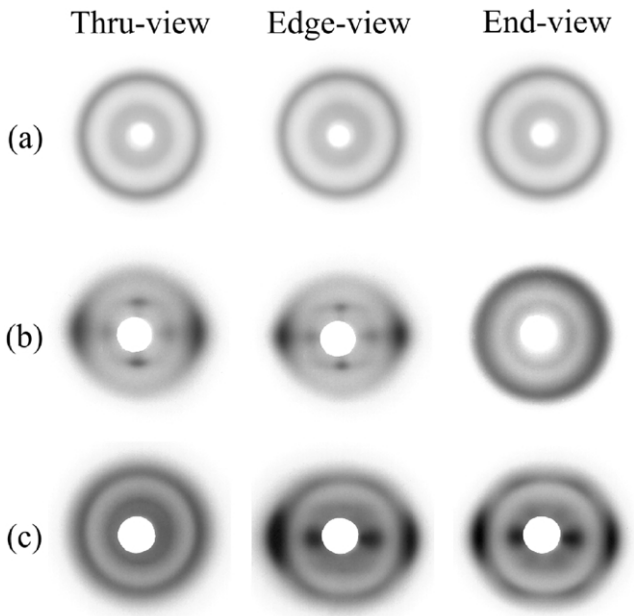


Fig. 2. Typical WAXD flat film patterns of polyamide 6 films before and after 65 °C stretching operation. (a) $\lambda_{TD}/\lambda_{MD} = 1.0 : 1.0$ (unstretched), (b) $\lambda_{TD}/\lambda_{MD} = 1.0 : 3.0$ and (c) $\lambda_{TD}/\lambda_{MD} = 2.5 : 3.0$.

almost '0' until $\lambda_{MD}$ reaches 2.5 and then slightly increases. For biaxially stretched films with $\lambda_{TD} > 1.0$, the $\Delta n_{23}$ decreases with $\lambda_{MD}$ even though the changes are not significant compared to the increases in $\Delta n_{12}$ and the $\Delta n_{13}$.

Fig. 9 shows changes in birefringences with respect to stretch temperature for $\lambda_{TD}/\lambda_{MD} = 1.0 : 3.0$ films. Both out-of-plane birefringences ($\Delta n_{13}$ and $\Delta n_{23}$) rapidly increase with respect to the stretch temperature while in-plane birefringence ($\Delta n_{12}$) stays almost constant for all stretch temperatures we used.

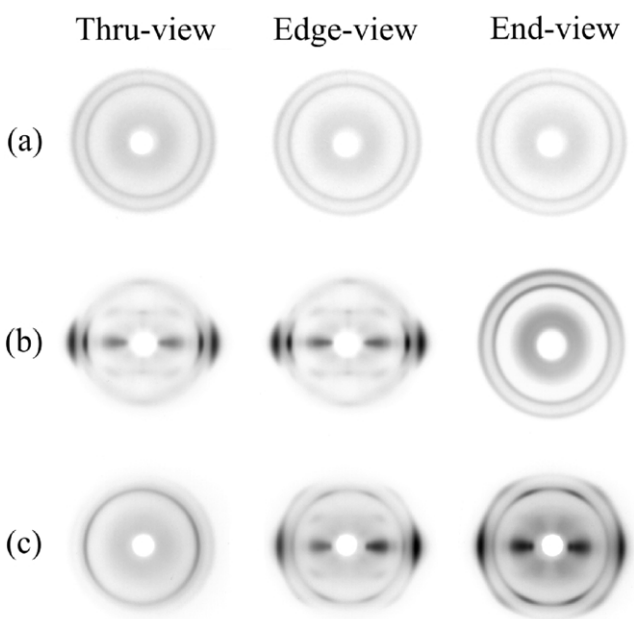


Fig. 3. Typical WAXD flat film patterns of the annealed polyamide 6 films which are unstretched or stretched at 65 °C before annealing. $\lambda_{TD}/\lambda_{MD} = 1.0 : 1.0$ (unstretched), (b) $\lambda_{TD}/\lambda_{MD} = 1.0 : 3.0$ and (c) $\lambda_{TD}/\lambda_{MD} = 2.5 : 3.0$.

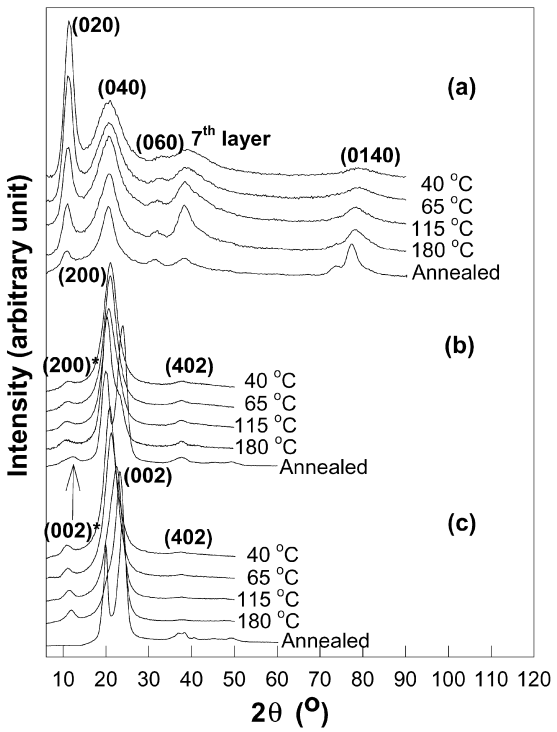


Fig. 4. WAXD $2\theta$ scans of polyamide 6 films stretched by $\lambda_{TD}/\lambda_{MD} = 1.0 : 3.0$ at various temperatures (from 40–180 °C). The reflections with a superscript '$*$' may result from harmonic reflections caused by X-ray beam of $\lambda = \lambda_{Cu\ K\alpha}/2$. The crystallographic planes to be concerned are aligned perpendicular to (a) the MD plane, (b) the TD plane, and (c) the ND plane.

Annealing the biaxial films, which were stretched at 65 °C, in a boiling 20% formic solution increased both out-of-plane birefringences ($\Delta n_{13}$ and $\Delta n_{23}$).

### 3.6. Mechanical properties

Fig. 10 presents mechanical properties of the unannealed extrusion cast polyamide 6 films which were stretched at 65 °C by various stretch ratios. The tests were carried out at room condition (21–25 °C and 25–31%RH). As shown in Fig. 10(a), the stress–strain behavior of unstretched extrusion cast film for all directions and stretched film ($\lambda_{TD}/\lambda_{MD} = 1.0 : 3.0$) for the TD exhibit a yield point, a long range plastic deformation, a strain hardening, and a failure. A change in test direction from the TD to the MD of this stretched sample results in an increase in yield stress and an eventual disappearance of the yield behavior, a gradual depression of the extent of plastic deformation and its eventual disappearance, and a large increase in tensile strength and a significant depression in elongation-at-break.

As shown in Fig. 11, the tensile strength for MD tests rises and the elongation-at-break for the same direction drops rapidly with increasing $\lambda_{MD}$. The test results vary in the opposite direction with respect to $\lambda_{TD}$. Most mechanical

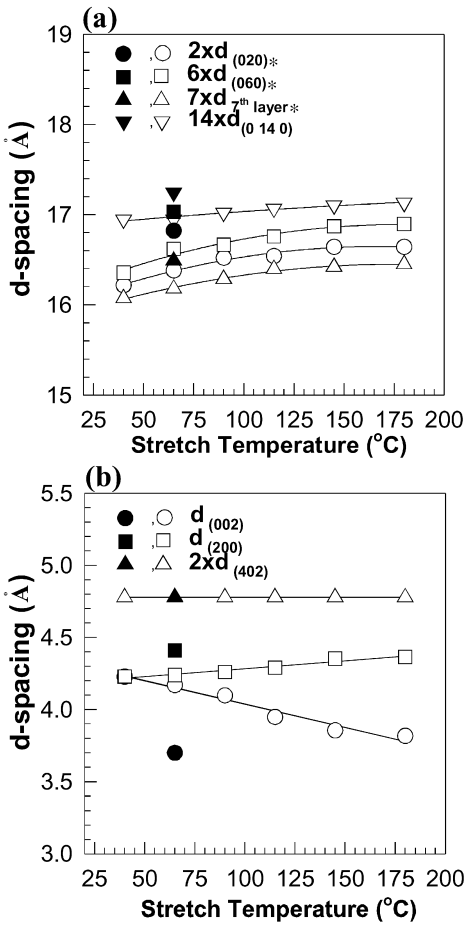


Fig. 5. *d*-spacings of polyamide 6 films stretched by $\lambda_{TD}/\lambda_{MD} = 1.0 : 3.0$ at various temperatures (from 40–180 °C). (a) For (0*k*0) reflections and (b) for (*h*0*l*) reflections. Open symbols: unannealed samples; closed symbols: annealed samples.

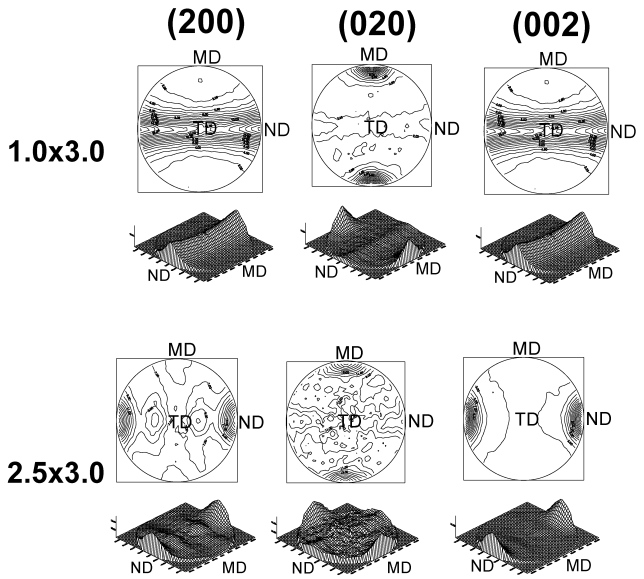


Fig. 6. Typical WAXD pole figure patterns (2D contour plots and 3D surface maps) of unannealed polyamide 6 films which are initially stretched at 65 °C by $\lambda_{TD}/\lambda_{MD}$.

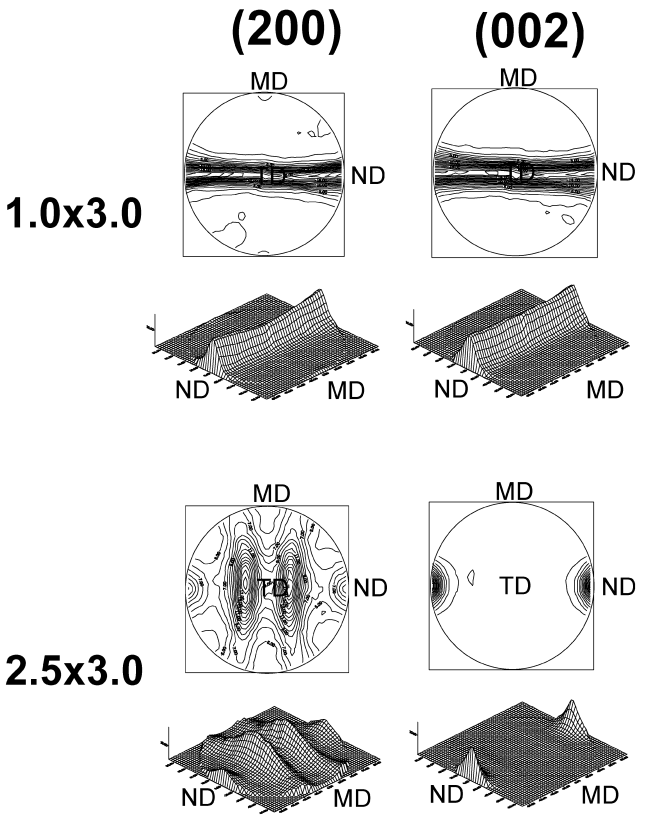


Fig. 7. Typical WAXD pole figure patterns (2D contour plots and 3D surface maps) of annealed polyamide 6 films which are initially stretched at 65 °C by $\lambda_{TD}/\lambda_{MD}$.

properties in TD tests behave in an opposite manner to those of the MD tests except that the elongation-at-break stays almost constant for unit width stretching ($\lambda_{TD} = 1.0$). Fig. 12 shows the effects of stretch temperature on the mechanical properties. Increasing stretch temperature for $\lambda_{TD}/\lambda_{MD} = 1.0 : 3.0$ samples improves tensile strength and depresses the elongation-at-break for both the MD and the TD.

## 4. Discussion and interpretation

### *4.1. Aging of the extrusion cast film*

We have shown with our DSC thermographs that extrusion cast polyamide 6 film can crystallize during storage at room condition (22–23 °C and 22–31%RH) if they are rapidly quenched into a highly amorphous state. This aging behavior involves initial depressions in both glass transition temperature and cold crystallization temperature followed by subsequent increases in both of them up to certain equilibrium values. The initial depressions seem to be caused by plasticization in amorphous phase by moisture absorbed from humid environment. We suspect the build-up of strong hydrogen bonds in the plasticized amorphous phase as the main driving force for producing

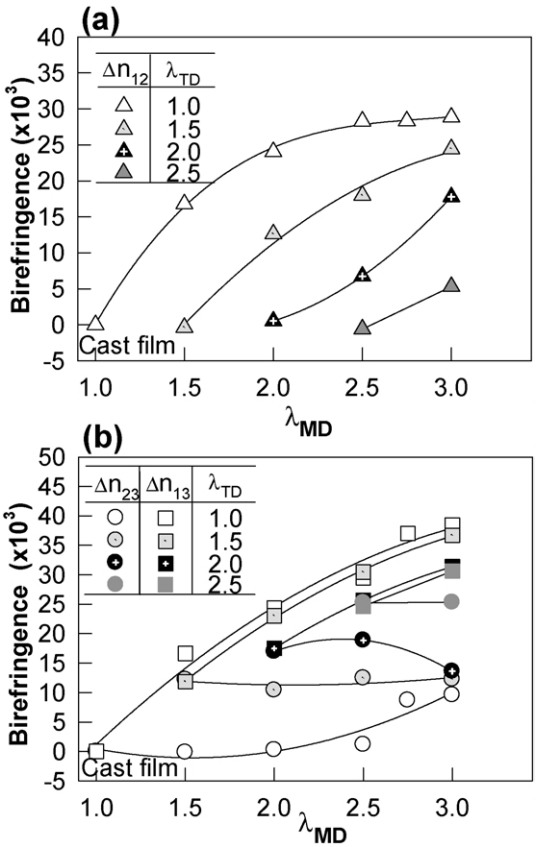


Fig. 8. Birefringences of the unannealed polyamide 6 films which are unstretched or stretched at 65 °C by various $\lambda_{TD}/\lambda_{MD}$. (a) In-plane birefringence and (b) out-of-plane birefringences.

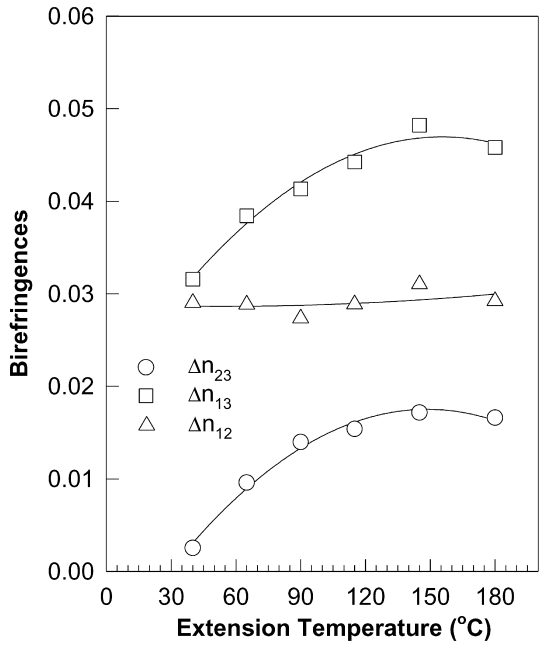


Fig. 9. Birefringences of the unannealed polyamide 6 films which are stretched by $\lambda_{TD}/\lambda_{MD} = 1.0 : 3.0$ at various temperatures (from 40–180 °C).

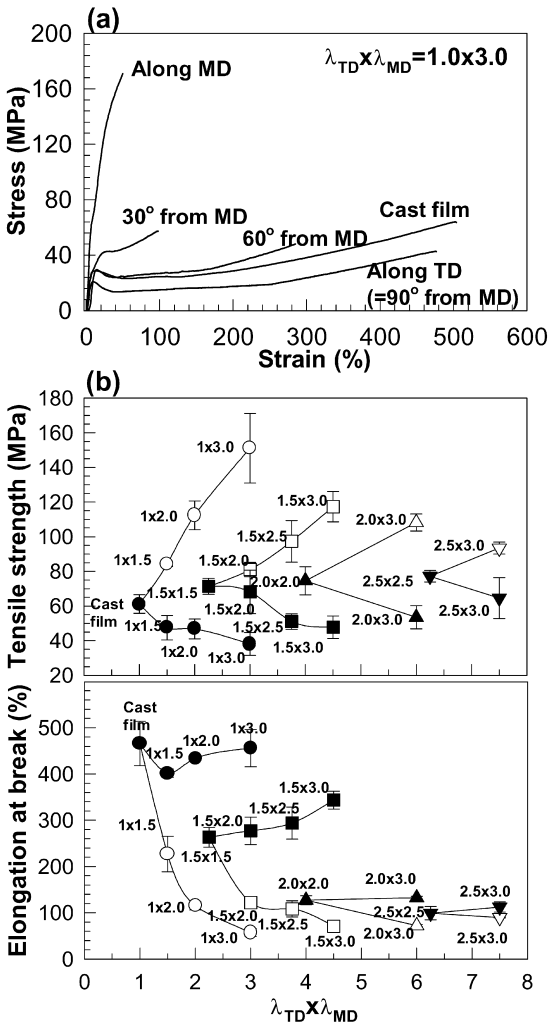


Fig. 10. Mechanical properties ((a) engineering stress versus strain (b) tensile strength (top) and elongation at break (bottom) in terms of stretch ratio ($\lambda_{TD}/\lambda_{MD}$); open symbols are the test results along the MD while closed symbols are those along the TD) of the unannealed polyamide 6 films which are stretched at 65 °C.

the increases in the glass transition temperature and cold crystallization temperature of them. We have observed similar aging behavior with extrusion cast polyamide 11 and 12 films as well as first bubble polyamide 612 films [36]. The polyamide 11 [39] and 12 [40] films were crystalline (crystallinity ≅ 20%) whereas the polyamide 612 films were highly amorphous (crystallinity ≅ 9%) at the initial stage of aging. Bankar et al. [21] found with WAXD patterns and birefringences that melt spun polyamide 6 fibers crystallize mostly on the bobbin into poorly defined β crystal during storage in a humid environment.

### *4.2. Crystal structure and polymorphism in polyamide 6 films*

The crystal structure of polyamide 6 has been extensively studied [1,4–6,9,10,12–14,20–23]. As we discussed in the introduction, room temperature crystals of polyamide 6 can

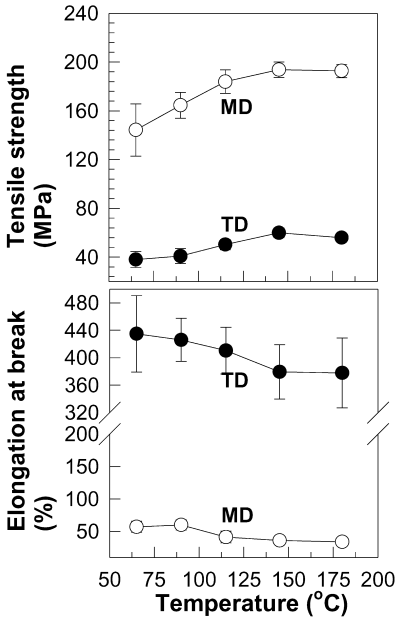


Fig. 11. Mechanical properties of the unannealed polyamide 6 films which are stretched by $\lambda_{TD}/\lambda_{MD} = 1.0 : 3.0$ at various temperatures (from 40–180 °C).

be categorized into α [1,4,6], β [1,4,9,10] (or pleated α [22,23] and γ [5,13,14,18] unit cells with various sorts of intermediate states [12,20].

It is generally believed that melt spun polyamide 6 fibers crystallize into β [1,4,9,10] (or pleated α [22,23]) forms when they are aged and examined at room conditions. Similar to the γ crystal, the β (or pleated α) crystal was believed to have a unit cell of pseudo-hexagonal symmetry. The γ crystal is obtained by iodine treatment of the β (or pleated α) and the α crystals. The main difference of these two crystals is that the γ is not transformed to α crystals whereas the β is relatively easily done so. The WAXD flat film patterns of our extrusion cast films and films stretched at low temperature with unit width are similar to those of pseudo-hexagonal β (or pleated α) crystal of polyamide 6. If we carry out biaxial stretching at low temperature, the aged films exhibit poorly defined crystal but the symmetry is no longer pseudo-hexagonal but monoclinic. Rhee and White [32] have found that unannealed biaxially oriented double bubble polyamide 6 films formed by 65 °C stretching have poorly defined crystal which have characteristics of the well defined α crystal in their chain conformation and configuration (directionality of neighboring chains) as well as those of the γ crystal.

The room temperature crystal form of polyamides rapidly quenched from melt state can be altered depending on the annealing temperature [43–45]. In the case of polyamide 6, increasing the annealing temperature causes a continuous crystal transformation from poorly defined β (or pleated α) crystal to monoclinic α crystal. If the annealing is carried out above the Brill transition point followed by slow cooling, the (200) and (002) reflections can be obtained at

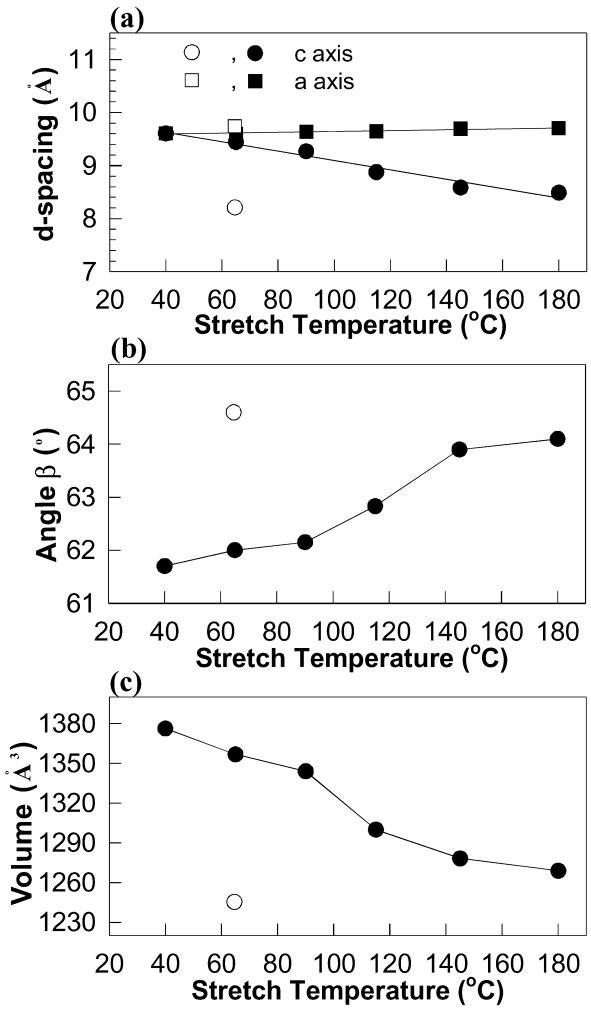


Fig. 12. Unit cell dimensions ((a) lengths of *a* and *c* axes (b) crystallographic β angle (c) volume) in terms of stretch temperature (from 40–180 °C) of the polyamide 6 films which are stretched by $\lambda_{TD}/\lambda_{MD} = 1.0 : 3.0$. Open symbols: annealed films; closed symbols: unannealed films.

about 4.4 and 3.7 Å, respectively, which are indicative of well-defined Brill–Holmes et al.'s α crystal. Fig. 12 shows changes in unit cell dimensions of polyamide 6 film stretched by $\lambda_{TD}/\lambda_{MD} = 1.0 : 3.0$ at various temperatures. This figure also includes the annealed state of the film which was originally stretched at 65 °C. The annealed film has *d*-spacings of Brill–Holmes et al.'s α crystal. According to Bankar et al. [21], a 20% formic acid solution is a good annealing medium with which well-developed α crystal is obtained. The length of the *a*-axis, which is parallel to the hydrogen bonding direction, is slightly increased from 9.6 Å at 40 °C with stretch temperature, and finally, reaches to about 9.8 Å after annealing. The percentage change is less than 2%. The length of the *c*-axis, another crystallographic axis perpendicular to the chain direction (*b*-axis), is shortened from 9.6 Å at 40 °C, and finally, reaches to 8.2 Å in the annealed films. The percentage shortening here is about 15%. The inter-planar angle β between (200) and

(002) crystallographic planes can be calculated from *d*-spacings of three lateral reflections such as (200), (002) and (402). The crystallographic β angle of monoclinic polyamide 6 crystal of these films increases with stretch temperature and becomes 64.6° after the annealing process. The 64.6° value for the annealed film is numerically close to the 65° of Brill's α structure.

Fig. 5(a) presents the effects of stretch temperature and solution annealing on $kd_{(0k0)}$ (chain axis repeat distance from (0*k*0) reflection). It is worthy to note that the values of $kd_{(0k0)}$ are inconsistent depending on the layer line of *k*. Similar behavior has been found with polyamide 6 [20,46,47], 11 [39], and 12 [48,49]. Wallner [46] argued that this unusual behavior results from mismatches in peak positions of the structure factor and Laue function in imperfect polyamide crystals which have long chain axis repeat distance. The usage of (0 14 0) planes was recommended for the calculation of chain axis repeat distance of polyamide 6 crystal [20,46,47]. The value of $14d_{(0\ 14\ 0)}$ of our films stretched by $\lambda_{TD}/\lambda_{MD} = 1.0:3.0$ increases with stretch temperature. It is 16.9 Å for 40 °C stretching and becomes 17.2 Å after being annealed in boiling 20% formic acid solution. The chain axis repeat distance of the annealed film is consistent with those of Brill–Holmes et al.'s α crystal. Double bubble polyamide 6 films also crystallize into α crystal by the same annealing process [32]. We have also observed that annealing oriented polyamide 612 [36] and 11 [39] films results in coexisting α and β crystals. The chain axis repeat distance of the unannealed films may be shortened from the all trans conformation of Brill–Holmes et al.'s α crystal due to rotations around single C–C bonds. As indicated in Fig. 12(c), both increasing stretch temperature and annealing give a large reduction of unit cell volume from 1376 $Å^3$ of 40 °C stretching to 1248 $Å^3$ of the annealed film whereas there exist increases in length of *a*- and *b*-axes as shown in Fig. 12(a) and Fig. 5(a) respectively.

### 4.3. Calculation of crystalline biaxial orientation factors

The level of biaxial orientation of biaxial polyamide 6 films containing monoclinic crystals was quantitatively evaluated with WAXD pole figure intensity data. The mean square cosine of a (*hkl*) plane can be calculated with *i*-direction centered pole figures through

$$\overline{\cos^2\Phi_{i,z}} = \overline{\cos^2\Phi_{i,[hkl]}} = \frac{\int_0^{\pi/2}\int_0^{2\pi} I_{hkl}(\kappa_{i,z},\Phi_{i,z})\cos^2\Phi_{i,z}\sin\Phi_{i,z}\,d\kappa_{i,z}\,d\Phi_{i,z}}{\int_0^{\pi/2}\int_0^{2\pi} I_{hkl}(\kappa_{i,z},\Phi_{i,z})\sin\Phi_{i,z}\,d\kappa_{i,z}\,d\Phi_{i,z}} \tag{4}$$

where $I_{hkl}(\kappa_{i,z},\Phi_{i,z})$ represents the intensity of reflection from (*hkl*) plane which is normal to *z* (or [*hkl*]) crystallographic axis at a position of longitudinal angle $\kappa_{i,z}$ and azimuthal angle $\Phi_{i,z}$.

In order to evaluate the level of chain axis orientation in biaxially oriented polyamide 6 films, two independent (*h*0*l*) reflections can be used. The (0*k*0) reflections may not be recommended since their intensities may be dependent on the crystal structure and perfection as well as the orientation. We found that only two lateral ((200) and (002)) reflections among (*h*0*l*) reflections were intensive enough for this purpose. Therefore, we have developed a pseudo-orthorhombic unit cell ($a'$ is normal to the hydrogen bonding plane, $c'$ is parallel to the chain axis, $b'$ is perpendicular to the $a'$–$c'$ plane). We have applied the same technique to polyamide 11 [37,38], 12 [37,40], and 612 [36] films. Table 2 lists the angles between the axes of the pseudo-orthorhombic unit cell and the poles from (*h*0*l*) crystallographic planes of the α unit cells we observed from our experiments. The mean-square cosines for the chain axis ($b$ or $c'$) and for the normal ($a'$) to the hydrogen bonding planes can be determined with $cos^2\Phi_{i,[00l]}$ and $cos^2\Phi_{i,[k00]}$ through

$$\overline{\cos^2\Phi_{i,c'}} = \frac{(f_1^2-e_1^2)\overline{\cos^2\Phi_{i,[00l]}} - (f_2^2-e_2^2)\overline{\cos^2\Phi_{i,[h00]}} + e_1^2f_2^2 - e_2^2f_1^2}{e_1^2(f_2^2-e_2^2) - e_2^2(f_1^2-e_1^2)} \tag{5a}$$

$$\overline{\cos^2\Phi_{i,a'}} = \frac{f_2^2\,\overline{\cos^2\Phi_{i,[h00]}} - f_1^2\,\overline{\cos^2\Phi_{i,[00l]}}}{f_2^2(e_1^2-f_1^2) - f_1^2(e_2^2-f_2^2)} \tag{5b}$$

where *i* denotes a principal stretch direction (the MD or the TD) of interest. The $e_1$ and $f_1$ are directional cosines of the [*h*00] and respective $a'$ and $b'$ axes. The $e_2$ and $f_2$ are those between [00*l*] (= a normal to hydrogen bonding (00*l*) plane) and $a'$ and $b'$ axes, respectively.

The resulting equations for the chain axis ($b$ or $c'$) and the normal to hydrogen bonding (00*l*) plane are

$$\overline{\cos^2\Phi_{i,c'}} = 1 - 1.2255\,\overline{\cos^2\Phi_{i,[200]}} - 0.7745\,\overline{\cos^2\Phi_{i,[002]}} \tag{6a}$$

$$\overline{\cos^2\Phi_{i,a'}} = \overline{\cos^2\Phi_{i,[002]}} \tag{6b}$$

White–Spruiell biaxial orientation factors [50] which are defined by

$$f^{B}_{MD,z} = 2\,\overline{\cos^2\Phi_{MD,z}} + \overline{\cos^2\Phi_{TD,z}} - 1 \tag{7a}$$

$$f^{B}_{TD,z} = 2\,\overline{\cos^2\Phi_{TD,z}} + \overline{\cos^2\Phi_{MD,z}} - 1 \tag{7b}$$

were utilized for biaxial orientation factors for $a'$ (= [002]), poles to α (200) planes (= [200]) and $c'$ (= $b$) crystallographic axes.

Table 2
Angles between axes ($a'$, $b'$ and $c'$) of an imaginary pseudo-orthorhombic unit cell and crystallographic plane normals ([$h0l$]) of a monoclinic α crystal of polyamide 6

| | $a'$ axis (°) | $b'$ axis (°) | $c'$ axis (°) |
|---|---|---|---|
| [002] | 0 | 90 | 90 |
| [200] | 64.6 | 25.4 | 90 |

### 4.4. Effects of stretching conditions on biaxial orientation factors

Fig. 13 presents the crystalline biaxial orientation factors of the extrusion cast polyamide 6 films which were stretched at 65 °C by various stretch ratios and subsequently annealed in boiling 20% formic acid solution for 20 min. The unstretched extrusion cast polyamide 6 film exhibited almost isotropic character ($f^{B}_{MD,c'} \cong 0, f^{B}_{TD,c'} \cong 0$). We raised $\lambda_{TD}$ from 1.0 to 2.5 at a constant $\lambda_{MD} = 3.0$ in order to investigate the influence of stretch ratio on the orientations of crystallographic axes. The levels of $a'$ axis (normal to hydrogen bonding plane) are designated as $f^{B}_{MD,a'}$ and $f^{B}_{TD,a'}$ for the MD and the TD, respectively. Increasing $\lambda_{TD}$ with $\lambda_{MD} = 3.0$ depresses both $f^{B}_{MD,a}$ and $f^{B}_{TD,a'}$ and makes them approach to the equal biaxially line (connecting $(0.5, 0.5)$ to $(-1, -1)$). This indicates that the more biaxial stretched films have the higher planarity of hydrogen bonding planes with respect to the film surface. $f^{B}_{MD,c'}$ and $f^{B}_{TD,c'}$ are indicative of the level of molecular chain orientation along the MD and the TD, respectively. Increasing $\lambda_{TD}$ with $\lambda_{MD} = 3.0$ results in a depression in $f^{B}_{MD,c'}$ and simultaneous improvement in $f^{B}_{TD,c'}$. This suggests an improvement in biaxiality (uniform distribution of chain molecules in the MD–TD plane) of crystal chain orientation.

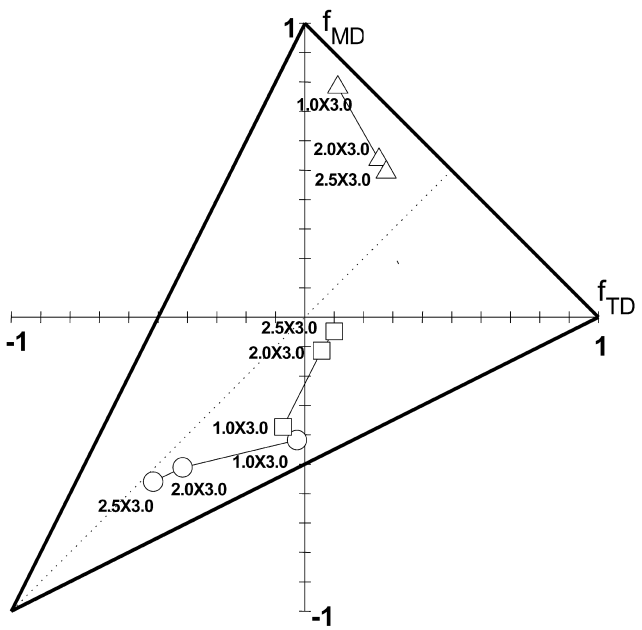


Fig. 13. White–Spruiell biaxial orientation factors for the annealed polyamide 6 films which are initially stretched at 65 °C by various $\lambda_{TD}/\lambda_{MD}$. (○) Normal to hydrogen bonding plane (= $a'$ axis); (□) poles to α (200) planes; (△) chain axis (= $c'$).

### 4.5. Mechanical properties versus out-of-plane birefringences

The mechanical properties of semi-crystalline thermoplastics were found to depend on the morphology such as crystal content and orientation of chain molecules. Mechanical properties such as young's modulus, tensile strength and elongation-at-break of melt-spun or drawn high density polyethylene [51], polypropylene [52–54], polyamide 6 [21,26] and polyamide 66 [55] fibers have been successfully correlated with the degree of molecular chain orientation. It would be convenient and useful to correlate the mechanical properties with birefringence, which measures the overall orientations in amorphous and crystalline regions. The modulus, tensile strength and elongation-at-break have been successfully correlated with birefringence for fibers of polypropylene [54], polyamide 6 [21,26] and 66 [55]. In the case of biaxially stretched films, we have found that the out-of-plane birefringence ($\Delta n_{ij}$) may be directly correlated with the level of orientation to the $i$ principal direction.

As clearly indicated in Fig. 14, the mechanical properties of the unstretched and stretched extrusion cast polyamide 6 films along a principal processing direction are well correlated with out-of-plane birefringence along the same direction. Fig. 14 shows a generalization of the correlation by including data from single bubble polyamide 6 films. The tensile strength increases and the elongation-at-break decreases, as the out-of-plane birefringence increases. Little change is found in tensile strength at low birefringence. The tensile strength shows increasingly significant rise as the birefringence increases. Depression of elongation-at-break is significant at low birefringence. When the out-of-plane birefringence exceeds about 0.04, the elongation-at-break levels off.

## 5. Conclusions

The crystal structure, orientation and mechanical properties of unannealed and annealed extrusion cast films have been studied before and after biaxial stretching. The unstretched extrusion cast polyamide 6 film which initially has about 5% crystallinity crystallizes spontaneously to a highly crystalline state having about 27% crystallinity during aging at room condition. This aging process involves significant changes in glass transition temperature, cold crystallization temperature and crystallinity with almost constant melting point. The excellent stretchability of the extrusion cast film disappears after the aging. Extrusion cast polyamide 6 films, which are either unstretched or stretched at low temperature, exhibit poorly defined β (pleated α)

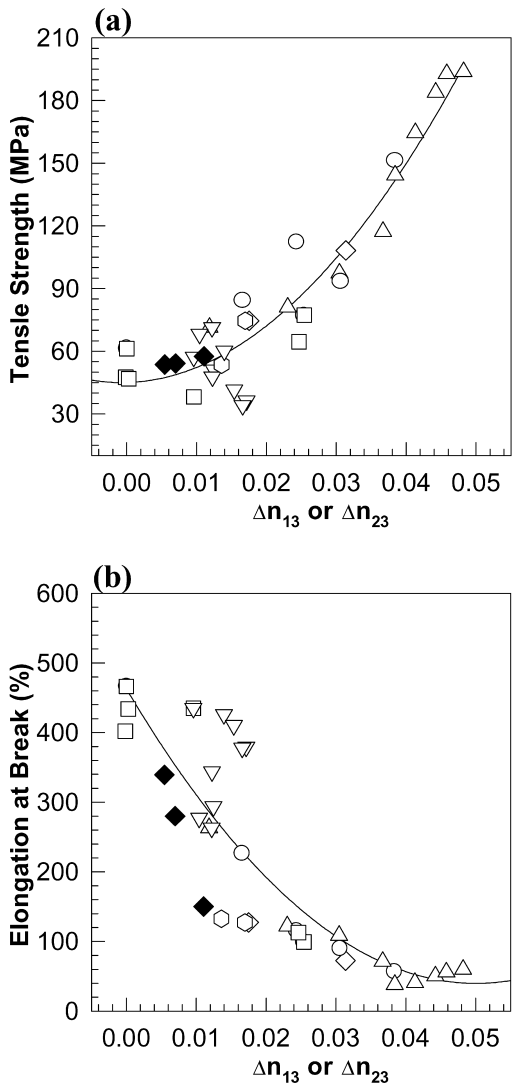


Fig. 14. Mechanical properties ((a) tensile strength (b) elongation-at-break) of polyamide 6 films in terms of out-of-plane birefringences. Open symbols: stretched extrusion cast films; closed symbols: single bubble films.

phase if they are cooled down to room temperature and aged for more than two weeks. The room temperature crystal form is transformed by increasing stretch temperature. At higher temperatures, the crystal becomes more like Brill–Holmes et al.'s monoclinic α form. However, even by 180 °C stretching, perfect α crystal is not obtained. Annealing the unstretched and stretched polyamide 6 films in boiling 20% formic acid solution leads to perfectly defined α crystal. The transition involves a separation of *d*-spacings for (002) and (200) planes, a reduction of (020) reflection intensity, and an elevation of *d*-spacing for the (020) plane. Dimensions of the α unit cell in the annealed films are significantly different from those of the β (pleated α) unit cell obtained by 40°C stretching. The *a*-axis, which is perpendicular to the chain axis and parallel to the hydrogen bonding plane, is slightly extended by less than 2% while the *c*-axis is shortened by about 15%. The extension of the *c*-axis is about 2%. The resulting volumetric shrinkage is about 9%.

White–Spruiell biaxial orientation factors for the crystallographic plane normals were calculated based on a newly developed imaginary pseudo-orthorhombic unit cell model. The anisotropy of the orientation is closely dependent upon the stretch ratio. Highly biaxially stretched films exhibit improved planarity of hydrogen bonding planes with respect to the film surface and more evenly distributing molecular chain axis orientation in the MD–TD plane. Mechanical properties (elongation-at-break and tensile strength) are successfully correlated with out-of-plane birefringences.

## References

[1] Brill R. Z Phys Chem B 1943;53:61–74.
[2] Bunn CW, Garner EV. Proc R Soc Lond 1947;A189:39–69.
[3] Aelion R. Ann Chim (Paris) 1948;3:5–61.
[4] Holmes DR, Bunn CW, Smith DJ. J Polym Sci 1955;17:159–77.
[5] Tsuruta M, Arimoto H, Ishibashi M. Kobunshi Kagaku 1958;15:619–27.
[6] Kinoshita Y. Makromol Chem 1959;33:1–20.
[7] Slichter WP. J Polym Sci 1959;36:259–66.
[8] Little KBr. J Appl Phys 1959;10:225–30.
[9] Ziabacki A. Kolloid Z 1959;167:132–41.
[10] Ziabicki A, Kedzierska K. J Appl Polym Sci 1959;2:14–23.
[11] Miyake A. J Polym Sci 1960;44:223–32.
[12] Roldan LG, Kaufman HS. J Polym Sci, Part B: Polym Lett Ed 1963;1:603–8.
[13] Vogelsong DC. J Polym Sci, Part A 1963;1:1055–67.
[14] Arimoto H, Ishibashi M, Hirai M, Chatani Y. J Polym Sci, Part A 1965;3:317–26.
[15] Sasaki T. J Polym Sci, Polym Lett Ed 1965;3:557–60.
[16] Northolt MG, Tabor BJ, Van Aartsen JJ. J Polym Sci, Part A-2 1972;10:191–2.
[17] Cojazzi G, Fichera AM, Garbuglio C, Malta V, Zannetti R. Makromol Chem 1973;168:289–301.
[18] Inoue K, Hoshino S. J Polym Sci, Polym Phys Ed 1973;11:1077–89.
[19] Newman BA, Sham TP, Pae KD. J Appl Phys 1977;48:4092–8.
[20] Parker JP, Lindenmeyer PL. J Appl Polym Sci 1977;21:821–37.
[21] Bankar VG, Spruiell JE, White JL. J Appl Polym Sci 1977;21:2341–58.
[22] Stepaniak RF, Carton A, Carlsson DJ, Wiles DM. J Appl Polym Sci 1979;23:1747–57.
[23] Stepaniak RF, Carton A, Carlsson DJ, Wiles DM. J Polym Sci, Polym Phys Ed 1979;17:987–99.
[24] Ishikawa T, Nagai S, Kasai N. J Polym Sci, Polym Phys Ed 1980;18:291–9.
[25] Kawaguchi A, Ikawa T, Fujiwara Y, Monobe K. J Macromol Sci, Phys Ed B 1981;20(1):1–20.
[26] Gianchandani J, Spruiell JE, Clark ES. J Appl Polym Sci 1982;27:3527–51.
[27] Owen AJ, Kollross P. Polym Commun 1983;24:303–6.
[28] Dosiere M, Point JJ. J Polym Sci, Polym Phys Ed 1984;22:1383–98.
[29] Kim KG, Newman BA, Scheinbeim JI. J Polym Sci, Polym Phys Ed 1985;23:2477–82.
[30] Jones NA, Atkins EDT, Hill MJ, Cooper SJ, Franco L. Polymer 1997;38:2689–99.
[31] Brill R. Makromol Chem 1956;18/19:294–309.
[32] Rhee S, White JL. Polym Engng Sci 1999;39:1160–75.
[33] Nagatosh F, Arakawa T. Polym J 1970;1:685–90.

[34] Penel-Pierron L, Depecker C, Seguela R, Lefebvre JM. J Polym Sci, Polym Phys Ed 2001;39:484–95.
[35] Penel-Pierron L, Seguela R, Lefebvre JM, Miri V, Depecker C, Jutigny M, Pabiot J. J Polym Sci, Polym Phys Ed 2001;39:1224–36.
[36] Rhee S, White JL. Int Polym Process 2001;16:272–84.
[37] Rhee S, White JL. Polym Engng Sci 2002;42:134–45.
[38] Rhee S, White JL. Polym Engng Sci 2002;42:889–98.
[39] Rhee S, White JL. J Polym Sci, Polym Phys Ed 2002; in press.
[40] Rhee S, White JL. J Polym Sci, Polym Phys Ed 2002;40:1189–200.
[41] Rhee S, White JL. Int Polym Process 2001;16:338–97.
[42] Inoue M. J Polym Sci, Part A 1963;1:2697–709.
[43] Biangardi HJ. J Macromol Sci, Part B: Phys 1990;29:139–53.
[44] Kyotani M, Mitsuhashi S. J Polym Sci, Part A-2 1972;10:1492–508.
[45] Hiramatsu N, Hashida S, Hirakawa S. Jpn J Appl Phys 1982;21: 651–4.
[46] Wallner LG. Monatsh Chem 1948;79:279–95.
[47] Kaji K, Sakurada I. J Polym Sci, Polym Phys Ed 1974;12:1491–7.
[48] Kaji K, Yamagishi H, Kitamaru D. Polym Prepr Jpn 1979;28:427.
[49] Shimizu J, Okui N, Tamaki S, Kikutani T, Takaku A. Seni Gakkaishi 1985;41:T513–20.
[50] White JL, Spruiell JE. Polym Engng Sci 1981;21:859–68.
[51] Dees JR, Spruiell JE. J Appl Polym Sci 1974;18:1053–78.
[52] Samuels RJ. J Polym Sci, Part A-2 1968;6:2021–41.
[53] Samuels RJ. J Macromol Sci, Phys 1970;4:701–59.
[54] Nadella HP, Spruiell JE, White JL. J Appl Polym Sci 1978;22(11): 3121–33.
[55] Danford MD, Spruiell JE, White JL. J Appl Polym Sci 1978;22(12): 3351–61.